Reviews in Cardiovascular Medicine

Rev. Cardiovasc. Med. **2022**; 23(2): 058
http://doi.org/10.31083/j.rcm2302058

Original Research

Coronary artery cavitation as a trigger for atherosclerotic plaque progression: a simplified numerical and computational fluid dynamic demonstration

Gianluca Rigatelli[1,*,†], Marco Zuin[2,†], Claudio Bilato[3], Thach Nguyen[4]

[1]Division of Cardiology, Department of Specialistic Medicine, Rovigo General Hospital, 45100 Rovigo, Italy
[2]Department of Translational Medicine, University of Ferrara, 44121 Ferrara, Italy
[3]Department of Cardiology, West Vicenza Hospital, 36014 Arzignano, Italy
[4]Cardiovascular Research, Methodist Hospital, Merrillville, IN 46410, USA
*Correspondence: jackyheart@libero.it (Gianluca Rigatelli)
[†]These authors contributed equally.

Academic Editor: Peter A. McCullough
Submitted: 23 July 2021 Revised: 19 October 2021 Accepted: 21 October 2021 Published: 12 February 2022

Abstract

Backgrounds: Coronary cavitation is supposed to be generated by both concentric and eccentric coronary artery stenosis which propagates downstream the vessel, creating microbubbles which exploded when the fluid pressure was lower than the vapor pressure at a local thermodynamic state. **Objective**: To assess, using numerical and computational fluid dynamic analysis (CFD), the potential of cavitation to both induce damage to coronary artery endothelium and to promote atherosclerotic plaque progression. **Methods**: We retrospectively reviewed the data 12 consecutive patients evaluated between 1st January 2013 and 1st January 2014 with an isolated hemodynamically significant Left Main (LM) disease. The patient specific geometries have been reconstructed. Bubble velocity has been calculated in accordance with Newton's second law. Both the forces arising from the bubbles' interaction with the continuous phase and impact with the endothelium have been evaluated. The impact of turbulence on the motion of bubbles have been modelled with a dispersion model. **Results**: Among the 12 patients retrospectively analysed [8 males, mean age 68.2 $\pm$ 12.8 years old], the mean LM stenosis was 72.3 $\pm$ 3.6%. As expected, in all subjects, LM stenoses induced cavitation which propagates downstream the vessel creating microbubbles. The higher concentration of vapor region was detected before the carina (within 0.8 to 1.3 cm from the stenosis). Due to the pressure gradient generated by the stenosis, formation of a re-entry jet which penetrates each bubble generated a shock wave. Before the carina, the mean bubbles radius observed was 4.2 $\pm$ 1.4 μm, which generated a mean peak pressure of 3.9 $\pm$ 0.5 MPa when they explode. **Conclusion**: The cavitation phenomenon is effectively generated in a model of LM bifurcation and instantaneous pressure-peaks due to collapses of vapor bubbles resulted in a measurable dynamic load on vessel wall potentially able to induce endothelial damage.

Keywords: Cavitation; Atherosclerosis; Plaque; Coronary artery disease

1. Introduction

Atherosclerosis is currently considered as an inflammatory and/or immunomodulatory reaction due to the presence of oxidized low-density lipoproteins (LDL) within the arterial wall concomitantly in the setting of traditional cardiovascular risk factors [1–4]. Nowadays, the triggers of coronary lesion progression and vulnerability from an asymptomatic fibro-atheromatous to a "vulnerable plaque" are not yet fully understood [5]. As we previously demonstrated, a rheological phenomenon called cavitation is generated by both concentric and eccentric coronary artery stenosis ($\geq$75% for the former and $\geq$50% for the latter) which propagates downstream the vessel, creating microbubbles which exploded when the fluid pressure was lower than the vapor pressure at a local thermodynamic state [6]. Biomechanically, cavitation might damage endothelial surfaces and promote thrombosis, as observed in subjects with left ventricular assist device (LVAD) [7]. In the present manuscript we sought to assess, using numerical and computational fluid dynamic analysis (CFD), the potential of cavitation to both induce damage to coronary artery endothelium and to promote atherosclerotic plaque progression.

2. Methods

2.1 Patient selection

We retrospectively analysed the data of 12 consecutive patients evaluated at Rovigo General Hospital between 1st January 2013 and 1st January 2014 reporting an isolated hemodynamically significant LM body/distal disease ($\geq$75% luminal narrowing on quantitative coronary angiography-QCA) [8]. Inclusion criteria were patients aged $\geq$18 years old with mild unprotected LM bifurcation disease diagnosed by both coronary computed tomography angiography (CCTA) and coronary angiography (CA). In all patients, QCA estimation (CAAS II 5.0 version; Pie Medical, Maastricht, The Netherlands) was used to assess the magnitude and characteristics of coronary artery disease

Copyright: © 2022 The Author(s). Published by IMR Press.
This is an open access article under the CC BY 4.0 license.

Publisher's Note: IMR Press stays neutral with regard to jurisdictional claims in published maps and institutional affiliations.

(CAD) on coronary angiography. Exclusion criteria were patients with previous CABG, diffuse CAD or any significant (≥50% luminal narrowing) stenoses of LAD, LCX or right coronary artery (RCA), considering that any other focal narrowing or diffuse coronary disease might have perturbed the coronary artery rheology, determining potential bias in the CFD analysis.

2.2 Coronary computed tomography and coronary angiography

The CCTA protocol has been already described [9]. Briefly, CCTA was acquired using a 64-slice multi-detector computed tomography scanner (64-detector row Lightspeed VCT scanner, GE Healthcare, Milwaukee, WI, USA). Electrocardiographic (ECG) gating was used for all scans. The scanning protocol was adjusted for patient weight and HR. Blood pressure was measured with an arm-band sphygmomanometer just before the examination. Each examination was independently interpreted by a trained CT radiologist using a combination of axial images, 3D volume-rendered images, multiplanar reformations, and maximum intensity projections. CA has been performed using a 6F radial approach whenever possible and bilateral angiographic 5F catheter. Angiographic data were independently reviewed by two 20-year experience angiographic operator (G.R. and L.R.). Any discordances were resolved via collegial discussion.

2.3 Computational models

As previously performed [9] the computational domain and patient specific geometries have been reconstructed using the open-source software package Vascular Modelling Toolkit (VMTK, https://www.vmtk.org), identifying the vessel centreline and then splitting the branches of the bifurcation. Therefore, external wall surfaces were reconstructed using circumferential cross sections perpendicular to the centrelines using the CAD software Rhinoceros 4.0 Evaluation (McNeel & Associates, Indianapolis, IN, USA) [10]. Atherosclerotic plaques have been modelled considering the distance between each node and the centreline of the external wall surface. Coronary artery stenosis (DS%) and minimal lumen area have been calculated considering the reconstructed coronary artery model. Specifically, the severity of the stenosis has been computed as 100% minus the percentage of minimal lumen area to the reference lumen area. Subsequently, the patient-specific geometries have been discretized using Ansys ICEM CFD (ANSYS Inc., Canonsburg, PA, USA) into linear tetrahedral volume elements which had a maximum size of 0.2 mm at the model surface. Meshing parameters included a default global maximal wall-face edge sizes of 1.0 and 0.15 mm, for the proximal length of both LAD and LCX (defined as the first fertile of the vessels lengths) and carina, respectively. Moreover, a mesh independence analysis was performed before the CFD simulation using the region adaptation function in FLUENT to refine the mesh until the modification in mesh size did not produce results with significant differences. A prism layer consisting of four layers with a height ratio of 1.2 was employed to capture the flow close to the lumen [9]. The mesh sizes used into these simulations were 280.090 elements and 45.375 nodes, respectively.

Blood has been modelled using a laminar non-Newtonian and incompressible fluid using the Navier–Stokes Eqn. 1

$$\rho \mathrm{v} \cdot \Delta \mathrm{v} = -\nabla \cdot \tau - \nabla \mathrm{P} \tag{1}$$

and the continuity Eqn. 2

$$\nabla \cdot \mathrm{v} = 0 \tag{2}$$

where v is the 3D velocity vector, P the pressure, ρ the density, and τ is the viscous stress tensor. Instead, the Casson model has been chosen to simulate the non-Newtonian fluid [11–13]. To maximize the fidelity of the CFD simulation, boundary conditions used for the simulation have been obtained from patient-specific data for the steady-state simulation. The patient-specific inlet velocity was acquired using the patient-specific stroke volume, determined as the difference between the end-diastolic (EDV) and end-systolic volumes (ESV), combined with the measured heart rate (HR), to achieve their time-averaged flow rate. A flow division has been contemplated at the two outlet boundaries represented by the end of LAD and LCX. The Murray's law was used to estimate the outflow for the side branches [14]. The model used to solve the governing equations was two-way coupled, implying that any deformation of blood vessel walls influences the fluid and vice versa [15]. Specifically, the motion of the vessel wall was mathematically described according to Toori *et al.* [16]

$$\rho \mathrm{w} = \frac{\delta \hat{} 2 \mathrm{u}(\ \mathrm{solid}\ )}{\delta \mathrm{t} \hat{} 2} - -\nabla \sigma(\ \mathrm{solid}\ ) = \rho \mathrm{W} * \mathrm{f}(\ \mathrm{solid}\ ) \tag{3}$$

where ρw is the wall density, f (solid represents the external body forces acting on the solid and σ (solid) is the a Cauchy stress tensor. The wall density of the artery was 960 kg/m^3 for the artery while for the cardiac muscle 1200 kg/m^3. The artery was assumed to be subjected to large strains and undergo deformations, resembling a hyperelastic neo- Hookean material. Simulations have been performed using the commercial software ANSYS FLUENT 14.0 (Ansys, Inc, Canonsburg, PA, USA).

Vapor has been modelled as discrete vapour bubbles whose trajectory is determined using a Lagrangian frame of reference [17]. Cavitation has been assumed to stary by cavitation nuclei which subsequently grow into bubbles undergoing different physical processes, which have been determined in a stochastic Monte-Carlo approximation [18].

The size of the nuclei has been sampled from a probability density function. When the pressure of blood fallen below its vapor pressure, the volume under tension was identified and the most probable locations for bubble nuclei formation were randomly calculated by sampling from a distribution function which considers the bubble volume fraction, volume and the non-dimensional tension of each Eulerian cell [19].

Bubble velocity has been calculated in accordance with Newton's second law. The forces arising from the bubbles' interaction with the continuous phase and impact with the endothelium have been also evaluated. The effect of turbulence on the motion of bubbles have been modelled with a dispersion model [20,21].

3. Results

During the study period, 15 patients were retrospectively identified. Of them, three were excluded due the presence of concomitant significant CAD. As a result, 12 consecutive patients [9 males, mean age 74.1 ± 6.3] were retrospectively analysed. The mean LM stenosis was 79.3 ± 3.6% (Table 1). As expected, in all subjects, LM stenoses induced cavitation which propagates downstream the vessel creating microbubbles followed either by explosion when the fluid pressure was lower than the vapor pressure at a local thermodynamic state or by recondensation when vapor structures were advected into areas of higher static pressure. The higher concentration of vapor region was detected before the carina (within 0.8 to 1.3 cm from the stenosis), as evidenced by the merged vapor regions showed in Fig. 1, Panel A, derived from the single analysis of all patients.

As expectable from the general cavitation theory, due to the pressure gradient generated by the stenosis as well as the relative turbulent flow, bubbles firstly increase their size (Fig. 1, Panels B1–B2) until their collapse above the vapor pressure level (Fig. 1, Panel B3). This event was promoted by the formation of a re-entry jet which penetrates each bubble (Fig. 1, Panel B4, red arrow) generating a shock wave and, if near the endothelium, transferring the related energy observed as an instantaneous pressure-peaks on the coronary surface. The bubble collapse happened quickly, after 2.1 ± 0.2 μs after achieving its maximus radius (Fig. 1, Panel B). Before the carina, the mean bubbles radius observed in the enrolled subjects was 4.2 ± 1.4 μm, which generated a mean peak pressure of 3.9 ± 0.5 MPa.

Table 1. Demographic and clinical characteristics of the patients enrolled to define the model.

	N = 12
	Mean or (%)
Age (years)	74.1 ± 6.3
Gender (Male) %	9 (75)
BMI (Kg/m^2)	27.3 ± 5.4
Overweight, %	7 (58.3)
Obese, %	1 (8.3)
SBP (mmHg)	140.5 ± 11.4
DBP (mmHg)	77.3 ± 9.8
HR (bpm)	82.2 ± 5.2
TC (mg/dL)	222.4 ± 12.1
TG (mg/dL)	168.3 ± 6.1
HDL (mg/dL)	32.3 ± 11.2
LDL-C	143.3 ± 10.5
Diabetes, %	6 (50)
HT, %	11 (91.6)
Lesion location on angiography	
-Ostial only	0 (0)
-Body	5 (41.6)
-Distal	7 (58.4)

BMI, body mass index; SBP, Systolic blood pressure; DBP, Diastolic blood pressure; HR, Heart rate; TC, Total cholesterol; TG, triglycerides; HDL, high density lipoprotein; LDL, Low density lipoprotein; IGF, Impaired fasting glucose; HT, arterial hypertension.

4. Discussion

The present study evaluates the relation between flow dynamics and cavitation phenomenon in promoting atherosclerotic plaque progression into coronary arteries. The results evidenced that shocks and instantaneous pressure-peaks, determined by the collapses of vapor bubbles, resulted in a measurable dynamic loads on endothelium which has the potential of causing damage or erosion. In this regard, CFD represents an important technique for providing non-invasive detailed blood flow data.

Obviously, the complexity of the mathematical analysis inherent to our demonstration has been simplified in order to be of practical value for the non-bioengineers professionals, maintaining the scientific quality of the analysis.

From a physical point of view, cavitation occurs when the pressure (P), in an area of flowing fluid, decreases below the level of vapor pressure (Pv). More precisely, cavitation bubbles form immediately below the (Pv) level, reaching the highest velocity at the lowest pressure level (Pmin), which is defined as vena contracta point. Subsequently, bubbles increase their size with the pressure increasing, leading to bubble collapse above the Pv level. This event represents the result of two different aspects, which form the essential substrates of cavitation: the former is characterized by a large pressure fluctuation (dp/dt), while the latter is due to the turbulent flow [22]. Conversely, the cavitation phenomenon in a hyperelastic or inhomogeneous soft solid occurs when in a neo-Hookean solid (which is an hyperleastic material model that can be used for predicting the non-linear stress-strain behaviour of materials undergoing deformation) under sufficient loading conditions

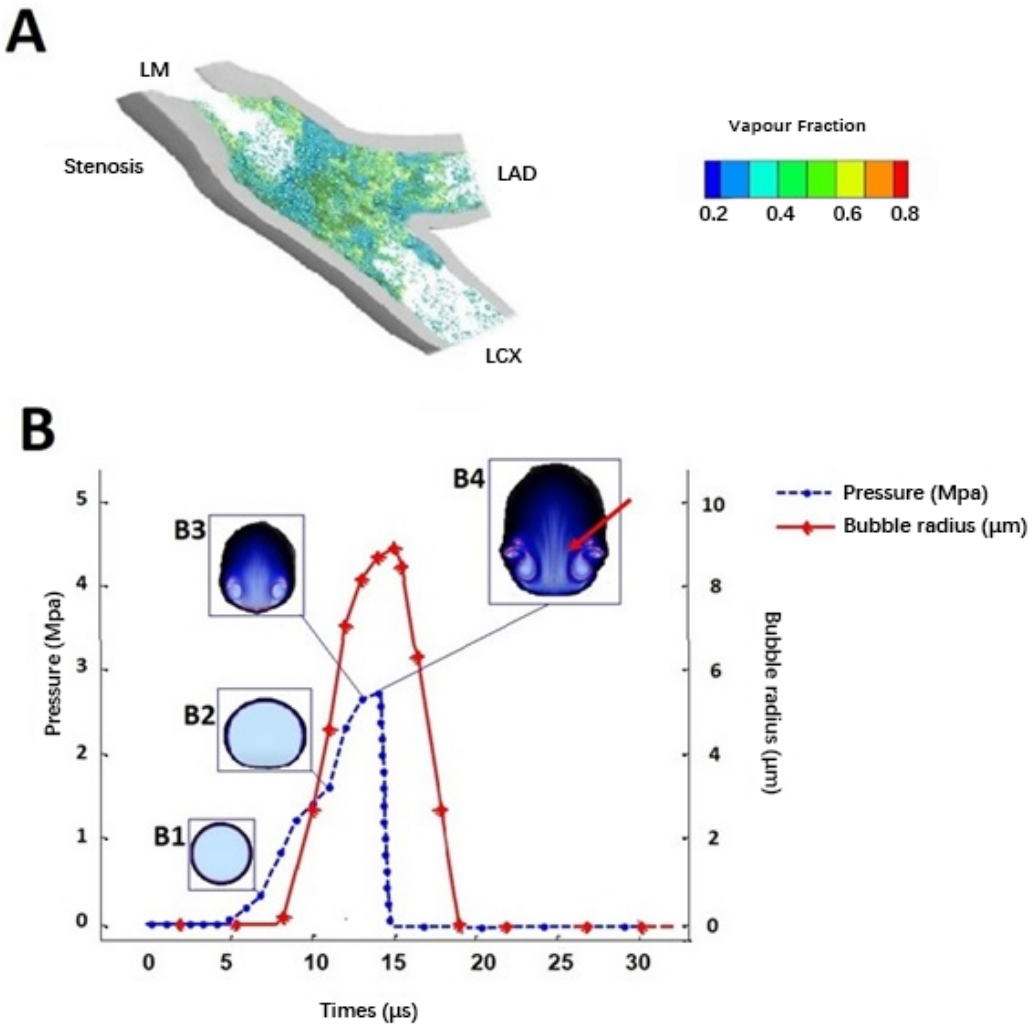

Fig. 1. Cavitation profile into a left main stenosis. (A) The simulation illustrates the vapor fraction iso-surfaces and the scattered bubble plots as predicted by the Langrangian model. Notably, most cavitation bubbles that form at the inlet of left main bifurcation do not collapse immediately but they are transported towards the vessel determining several interactions with the endothelium. (B) Graphical representation of the bubble radius modification and related pressure transmitted to the endothelium if the bubble collapse happened near to this last one. The magnification in boxes (B1–B4) evidences the dynamic modification of bubbles. The re-entry jet causing the collapse is evidenced with a red arrow.

with large triaxial forces cavities appear [23]. From a translational point of view, the cavitation within a fluid (e.g., blood) needs the presence of a significant vessel stenosis to be generated while the cavitation of the hyperelastic material (e.g., the atherosclerotic plaque) needs sufficient triaxialities to be generated.

The hypothesis that the energy released by microbubbles collapse on the plaque surface be able to produce a significant destabilization of the plaque, promoting cardiovascular events, is similar to the findings reported some years before, regarding the occurrence of haemolysis and generation of valvular lesions, due to the cavitation, observed in patients with MHVs [24]. The cavitation phenomenon, alone, is not able to explain the growth as well as the structural and biochemical modifications of the coronary atherosclerotic plaque but may act as a concurrent rather a causal factor in the precipitation of the atherosclerotic disease. Indeed, the cavitation is observed in bloodstream, in accordance to the fluid dynamic laws, only when a significant abrupt stenosis [6,25], even concentric or eccentric, determines the sudden decrease of P below the Pv [26]. Similarly, when the cavitation is analysed into the plaque, which has been compared to a soft inhomogeneous solid, requires a specific loading conditions to become significant and able to determine the "failure" of the plaque [27]. Intriguingly, some studies have evidenced that the cavitation can be used to induce a localized and controlled atherosclerotic process in the abdominal aorta [28].

Doubtless, due the relative few number of patients enrolled and considering the peculiar location of the stenotic

lesion as well as the distance to the carina, and the bifurcation angle, which may significantly vary among patients, our preliminary data must be cautiously considered since their integration into may have led to some intrinsic bias.

The cavitation phenomenon probably produces a specific rheologic effect which contribute to plaque progression. In other words, the lesion induced by long-lasting and continuous explosion of bubbles colliding with the endothelium may transfer enough energy to the vessel wall to generate an endothelial injury which triggered the progression of the plaque by the well-known cascade.

5. Limitations

Our study suffers from several intrinsic limitations which firstly include its retrospective single center small patients sample nature. Secondly, the application of a phenomena that usually produces erosion on different surface than the endothelial wall of the coronary tree. Thirdly, we considered a diastolic steady flow for the analysis: in coronary vascular tree the flow is mainly diastolic with a small systolic compound and we cannot avoid a mild model distortion induced by this latter flow component. Fourthly the plaque has not been characterized in its components, fibrous, fibrous -fatty, necrotic core, calcified, because of the huge number of different model combinations which would make the analysis inconsistent. Finally, the absence of a histological confirmation of the damage which obviously cannot be made *in vivo*.

6. Conclusions

Our study demonstrated by means of numerical and CFD analysis that in coronary model of LM bifurcation with a significant disease, the cavitation phenomena is effectively generated and instantaneous pressure-peaks due to collapses of vapor bubbles resulted in dynamic loads on endothelium which reached a measurable mean pressure of 3.9 MPa, which may have the potential to provoke endothelial damage. This demonstration offers the basis for further experimental studies about the significance of cavitation in coronary plaque progression.

Author contributions

GR—Conceptualization; write the manuscript; reviewed the manuscript; data analysis; supervision; MZ—Conceptualization; write the manuscript; reviewed the manuscript; data analysis; CB—Critical revision and final supervision; TN—Conceptualization; write the manuscript; reviewed the manuscript; data analysis.

Ethics approval and consent to participate

Ethical approval was waived due to the retrospective nature of the study. All partecipants provide the consent to partecipate to the study.

Acknowledgment

Not applicable.

Funding

This research received no external funding.

Conflict of interest

The authors declare no conflict of interest.

References

[1] Wilensky RL, Shi Y, Mohler ER, Hamamdzic D, Burgert ME, Li J, *et al*. Inhibition of lipoprotein-associated phospholipase a2 reduces complex coronary atherosclerotic plaque development. Nature Medicine. 2008; 14: 1059–1066.

[2] Wilensky RL, Hamamdzic D. Molecular basis for the vulnerable plaque: potential therapeutic role for immunomodulation. Current Opinion in Cardiology. 2007; 22: 545–551.

[3] Maiolino G, Rossitto G, Caielli P, Bisogni V, Rossi GP, Calò LA. The Role of Oxidized Low-Density Lipoproteins in Atherosclerosis: the Myths and the Facts. Mediators of Inflammation. 2013; 2013: 714653.

[4] Fruchart J, Nierman MC, Stroes ESG, Kastelein JJP, Duriez P. New Risk Factors for Atherosclerosis and Patient Risk Assessment. Circulation. 2004; 109: III15-9

[5] Virmani R, Kolodgie FD, Burke AP, Finn AV, Gold HK, Tulenko TN, *et al*. Atherosclerotic plaque progression and vulnerability to rupture: angiogenesis as a source of intraplaque hemorrhage. Arteriosclerosis, Thrombosis, and Vascular Biology. 2005; 25: 2054–2061.

[6] Rigatelli G, Zuin M, Ngo TT, Nguyen HT, Nanjundappa A, Talarico E, *et al*. Intracoronary cavitation as a cause of plaque rupture and thrombosis propagation in patients with acute myocardial infarction: a computational study. Journal of Translational Internal Medicine. 2019; 7: 69–75.

[7] Zuin M, Rigatelli G, Braggion G, Bacich D, Nguyen T. Cavitation in left ventricular assist device patients: a potential early sign of pump thrombosis. Heart Failure Reviews. 2020; 25: 965–972.

[8] Chen S, Sheiban I, Xu B, Jepson N, Paiboon C, Zhang J, *et al*. Impact of the Complexity of Bifurcation Lesions Treated with Drug-Eluting Stents: the DEFINITION study (Defnitions and impact of complEx biFurcation lesIons on clinical outcomes after percutaNeous coronary IntervenTIOn using drugeluting steNts). JACC: Cardiovascular Interventions. 2014; 7: 1266–1276.

[9] Zuin M, Rigatelli G, Vassilev D, Ronco F, Rigatelli A, Roncon L. Computational fluid dynamic-derived wall shear stress of non-significant left main bifurcation disease may predict acute vessel thrombosis at 3-year follow-up. Heart and Vessels. 2020; 35: 297–306.

[10] Rigatelli G, Zuin M, Dell'Avvocata F, Nguyen T. Rheolytic efects of left main mid-shaft/distal stenting: a computational fow dynamic analysis. Therapeutic Advances in Cardiovascular Disease. 2018; 12: 161–168

[11] Morlacchi S, Colleoni SG, Cárdenes R, Chiastra C, Diez JL, Larrabide I, *et al*. Patient-specifc simulations of stenting procedures in coronary bifurcations: two clinical cases. Medical Engineering & Physics. 2013; 35: 1272–1281

[12] Theodorakakos A, Gavaises M, Andriotis A, Zifan A, Liatsis P, Pantos I, *et al*. Simulation of cardiac motion on non-Newtonian, pulsating fow development in the human left anterior descending coronary artery. Physics in Medicine and Biology. 2008; 53: 4875–4879

[13] Shibeshi S, Collins W. The rheology of blood fow in a branched arterial system. Applied Rheology. 2005; 15: 398–405
[14] Murray CD. The physiological principle of minimum work. the vascular system and the cost of blood volume. Proceedings of the National Academy of Sciences of the United States of America. 1926; 12: 207–214
[15] Wang Y, Quaini A, Čanić S. A Higher-Order Discontinuous Galerkin/Arbitrary Lagrangian Eulerian Partitioned Approach to Solving Fluid–Structure Interaction Problems with Incompressible, Viscous Fluids and Elastic Structures. Journal of Scientific Computing. 2018; 76: 481–520.
[16] Torii R, Keegan J, Wood NB, Dowsey AW, Hughes AD, Yang G, *et al*. The effect of dynamic vessel motion on haemodynamic parameters in the right coronary artery: a combined MR and CFD study. The British Journal of Radiology. 2009; 82: S24–S32.
[17] Rapp BE. Microfluidics: Modelling, Mechanics and Mathematics. In Micro and Nano Technologies. Elsevier. Amsterdam, Netherlands 2017.
[18] Liang F. An Overview of Stochastic Approximation Monte Carlo. Wiley Interdisciplinary Reviews: Computational Statistics. 2014; 6: 240–254.
[19] Martínez-Bazán C, Montañés JL, Lasheras JC. Statistical description of the bubble cloud resulting from the injection of air into a turbulent water jet. International Journal of Multiphase Flow. 2002; 28: 597–615.
[20] Moss WC, Levatin JL, Szeri AJ. A New Damping Mechanism in Strongly Collapsing Bubbles. Proceedings: Mathematical, Physical and Engineering Sciences. 2000; 456: 2983–2994.
[21] Martínez-Bazán C, Montañés J, Lasheras J. On the breakup of an air bubble injected into a fully developed turbulent flow. Part 1. Breakup frequency. Journal of Fluid Mechanics. 1999; 401: 157–182.
[22] Nguyen Thach N, Nguyen Nhan Minh T, Truong Vien T, Vo Viet M, Rigatelli G. Cavitation Phenomenon Creating Bubbles and Their Explosion in the Coronary Arteries Caused Damage to the Endothelium and Start the Atherosclerotic Process. Journal of the American College of Cardiology. 2018; 71: A269.
[23] Kang J, Wang C, Tan H. Cavitation in inhomogeneous soft solids. Soft Matter. 2018; 14: 7979–7986.
[24] Girod G, Jaussi A, Rosset C, De Werra P, Hirt F, Kappenberger L. Cavitation versus degassing: in vitro study of the microbubble phenomenon observed during echocardiography in patients with mechanical prosthetic cardiac valves. Echocardiography. 2002; 19: 531–536.
[25] Nguyen T, Dang T, Nguyen TN, Anh CH, Le Huy Hoang P, Darwish T, *et al*. GW29-e0862 NEW DISCOVERY: Gas Bubbles Rupture in the Coronary Arteries is most Likely the Mechanism Breaking the Thin Cap of Plaques Causing Acute Coronary Syndrome. Journal of the American College of Cardiology. 2018; 72: C105.
[26] Johansen P. Mechanical heart valve cavitation. Expert Review of Medical Devices. 2004; 1: 95–104.
[27] Maldonado N, Kelly-Arnold A, Cardoso L, Weinbaum S. The explosive growth of small voids in vulnerable cap rupture; cavitation and interfacial debonding. Journal of Biomechanics. 2013; 46: 396–401.
[28] Zong YJ, Wan JJ, Qiao YZ, Li WS, Zou XR, Wan MX. Cavitation Endothelium Damage of Large Artery Vessel: a Potential Application to Animal Model of Atherosclerosis. IFMBE Proceedings. 2014; 42: 63–66.